




Nonsymmetrical thermal conductivity along the director field in ferroelectric nematic liquid crystals

Lidiane Maria de Souza ¹, Junaid Sofi ², and Erms Pereira ^{1,*}

¹*Department of Physics, Federal Rural University of Pernambuco, Recife 52171-900, Brazil*

²*Soft Matter Physics Group, School of Physics and Astronomy, University of Leeds, Leeds LS2 9JT, United Kingdom*



(Received 5 October 2023; accepted 6 August 2024; published 9 September 2024)

The synthesis of ferroelectric nematic liquid crystals (FNLCs) concludes the long wait for their existence and potential usage in multiple liquid crystal based applications. In FNLCs, electric polarization in the nematic phase significantly decreases the switching time of in-on display pixels. In this article, we report the occurrence of translation symmetry breaking for heat propagation along the director field \hat{n} in the ferroelectric nematic phase. Due to the $C_{\infty V}$ symmetry of such a phase and close similarity to the bent-core polar liquid crystal phase, a rank-3 tensor describes its scalar order parameter and algebraic deductions. The finite element simulations show the occurrence of the nonsymmetrical thermal conductivity along \hat{n} . The preferential heat transport in FNLCs can allow them to work as an all-thermal monophasic non-nanostructured single-material thermal rectifier. We expect that this study will contribute towards the FNLCs application as functional layers and inks.

DOI: [10.1103/PhysRevE.110.034703](https://doi.org/10.1103/PhysRevE.110.034703)

I. INTRODUCTION

Liquid crystals (LCs) have long captivated the scientific community, presenting a unique interplay between the characteristics of conventional liquids and solid crystals [1–3]. Particularly in display technology [4], the nematic liquid crystals (NLCs) play a central role wherein the NLC molecules uniformly align along an average orientation defined by the director field \hat{n} , and altered by an applied field [5]. The need for faster switching times under applied field in LC displays encouraged the synthesis of ferroelectric nematic liquid crystals (FNLCs). The FNLCs are especially interesting for their low-energy operability in display applications and have the potential to emerge as a standout subset within the diverse class of LCs [6–8]. In the ferroelectric nematic phase, the spontaneous polarization of the nematic (fluidlike) phase can be reversed by applying an electric field [9]. Such a distinctive feature of molecules makes the FNLCs potential candidates for multiple technological applications. From display technology [10] and advances in data storage [11,12] to innovations in optoelectronics [9,13], the potential of FNLCs remains vast and largely untapped.

Moreover, FNLCs have demonstrated potential in manipulating droplets using light and heat [14,15]. In the context of light-driven movement, a laser beam creates a nonuniform electric field around the FNLC droplet, compelling it to move via dielectrophoresis [16]. Conversely, when heat is the driving force, ionic contaminants undergo rotation due to the combined effects of a vertical thermal gradient, pyroelectricity, and ferronematicity. However, such applications use the direct electric interaction with the spontaneous

polarization in the nematic phase, without exploring other physics in FNLCs due to the absence of further properties in FNLCs.

In this article, we report on the nonsymmetrical propagation of heat in the ferroelectric nematic phase. The distinct intramolecular mass distribution that produces a $C_{\infty V}$ symmetry group in FNLC molecules [17,18] (see Fig. 1), exemplified by DIO [19] and RM734 [20,21], enables us to characterize their order parameter tensor using rank-3 tensors, drawing parallels with the polar phase of bent-core liquid crystals [22]. We conclusively demonstrate the translation symmetry-breaking nature of heat flux within the ferronematic phase through both algebraic analysis and the finite element simulations by employing the rank-3 tensor that represents the ferronematic phase $C_{\infty V}$ symmetry group.

II. MODEL AND FORMALISM

Ferroelectric nematic liquid crystals are described by scalar order parameter tensors Q that depends on the director vector field \hat{n} and the polar vector \mathbf{p} [23], elements linked to the system's symmetry [7]. The director field \hat{n} defines the local average molecular alignment in space. The thermal conductivity in the nematic phase of rodlike molecules with $\hat{n} = \mathbf{p}/|\mathbf{p}|$ relates to the thermal conductivity tensor as $k_o = k_{\text{iso}}I + k_{\text{aniso}}Q$, where $k_{\text{iso}} = (k_{\parallel} + 2k_{\perp})/3$, I is the identity tensor, $k_{\text{aniso}} = k_{\parallel} - k_{\perp}$, and k_{\parallel} and k_{\perp} are the parallel and perpendicular thermal conductivity parameters relative to the molecule's major axis, respectively [24–26]. This tensor rules the Fourier law for the heat conduction by $q^i = -k^{ij}T_j$, where q^i are the components of the heat flux q , k_o^{ij} are the components of the ordinary rank-2 thermal conductivity tensor k_o , T is the temperature, and $T_k \equiv \frac{\partial T}{\partial x^k}$.

*Contact author: erms.pereira@ufrpe.br

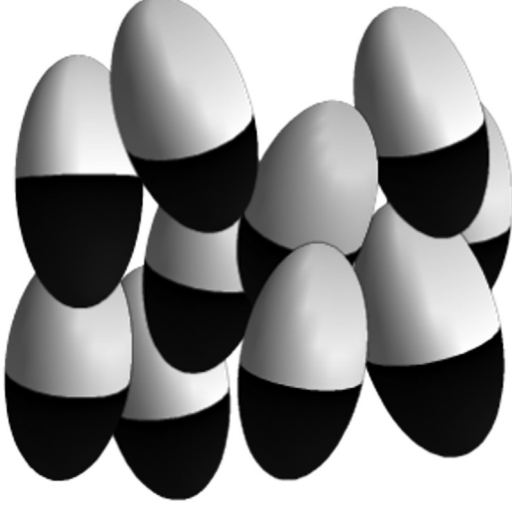


FIG. 1. Example of ellipsoid molecules with director \hat{n} and polar vectors $\hat{p} = \hat{n} = \hat{z}$, and a polar mass molecular distribution, where the black and white areas represent the greater and lesser mass densities, respectively.

III. RESULTS AND DISCUSSION

A. Polar effects from the rank-3 approach on the Fourier equation

Hard-core interactions, rather than electric dipole ones, describe the phase transition of ordinary rodlike nematic liquid crystals [27]. Under these sterielike interactions, we use the mass moment tensor as the order parameter. Since the polar mass distribution in the molecule of the NLCs produces the $C_{\infty V}$ symmetry [17,18], we propose that describing the mass moment tensor with high-order tensorial elements in FNLCs is a more suitable approach. Proceeding with a multipolar expansion of the mass moment tensor up to the octupolar element using spherical harmonics [28], this term can be split in a vector and in the rank-3 symmetric traceless tensor. The tensor that represents the $C_{\infty V}$ symmetry for the polar phase V [17,18] is [22]

$$A^{ijk} = \sqrt{\frac{5}{2}} \left(n^i n^j n^k - \frac{1}{5} (\delta^{ij} n^k + \delta^{jk} n^i + \delta^{ki} n^j) \right),$$

where \hat{n} is the unitary director field. Thus, the thermal conductivity tensor k^{ij} in Fourier's law for heat conduction, $q^i = -k^{ij} T_j$ will be as follows:

$$k^{ij} = k_o^{ij} + a_0 A^{ijk} T_k,$$

where q is the heat flux, k_o^{ij} are the components of the ordinary rank-2 thermal conductivity tensor k_o , T is the temperature, $T_k \equiv \frac{\partial T}{\partial x^k}$, and the parameter a_0 preserves the physical units.

Ordinarily, the nonlinear parts of the heat conductivity are small because the liquid crystalline molecules have minor variations from the mass homogeneous rod. Since the polar mass distribution of the FNLC molecules is responsible for producing the $C_{\infty V}$ polar symmetry [17,18], the FNLC demands the octupolar approach using rank-3 tensors. In our work, the nonlinear effects are consequences of the FNLC's polar mass distribution instead of the slight deviations of the

mass as observed in otherwise homogeneous rodlike nematic liquid crystal molecules.

B. Polar phase rectifies heat

Thermal rectifiers have the translation symmetry breaking for heat conduction along one axis as their fundamental feature, with the forward direction along this axis being the one with the highest thermal conductivity [24,25,29–37]. There are multiple methods to achieve such a nonsymmetric thermal conductivity. For instance, one can load material at one end of carbon nanotubes or cut graphene sheets with anisotropic shapes [31,32], explore the phase transition of molybdenum disulfide (MoS_2) [33], or use the radiative heat transfer between two nanoparticles applying an electric field [34]. Among the nematic liquid crystals, the thermal rectifier can be achieved by distorting the director field \hat{n} to a special configuration [24,35–37]. However, most of these examples need a multistep manufacturing process to produce the desired thermal rectifier. Here, we study the heat conduction in FNLCs in their spontaneous polar phase.

Regarding q_R , the heat flux in the reverse direction (the one with the least thermal conductivity), and q_F , the heat flux in the forward direction (the one with the highest thermal conductivity), one identifies which are such directions using Fourier's law noting that $q_R < q_F$. Also, considering $\hat{n} = +\hat{x}$, one has $A^{xxx} = A^{zzz} = 0$, $q^y = q^z = 0$,

$$q^x = - \left(k_o^{xx} + \frac{a_0}{5} \sqrt{10} T_x \right) T_x,$$

and

$$q^x = \left(k_o^{xx} - \frac{a_0}{5} \sqrt{10} T_x \right) T_x$$

when $\nabla T = T_x (+\hat{x})$ and $\nabla T = T_x (-\hat{x})$, respectively. Defining $\hat{n} = \hat{p}$ due to the invariance of the elastic energy relative to the director n , one concludes that, when $\hat{p} = \hat{x}$, the forward direction is $-\hat{p}$, while the reverse one is $+\hat{p}$. With this result, the FNLC can compound a thermal rectifier film to be applied on glass windows [37], and we also have a thermal way to determine the direction of \hat{p} : $\hat{p} = \hat{q}_R$.

The resultant nonlinear dependence on the heat flux is similar to that of the periodic structures, which also envisages them to be used as thermal rectifiers [38]. In periodic structures case, a host material with periodic inclusions produces an effective thermal conductivity of $k_{\text{eff}} = k_{\text{linear}} + k_{\text{nonlinear}} T^\alpha$, where k_{linear} is the linear contribution, $k_{\text{nonlinear}}$ is the magnitude of the nonlinear part, and α is an adjustment parameter. Another example, but at the microscopic level, is when one suggests exotic interactions between the oscillators' Hamiltonian, allowing us again to set specific parameters that could rectify heat.

C. Thermal aspects of the simulations

Since there is no comprehensive molecular statistical theory of heat conduction in liquid crystals, and this property has only been measured in a few materials [41], we focused on the consequences that the rank-3 approach produces on the thermal conductivity and the partial differential equations of Fourier's law. The simulations using the finite element shows

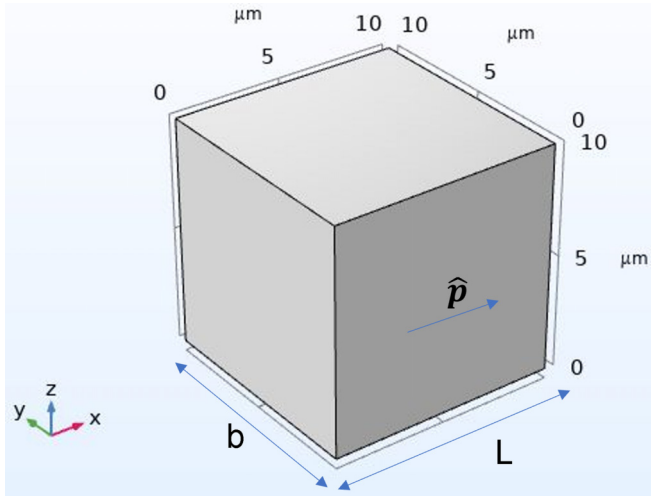


FIG. 2. Simulation region of length 10 μm , with polar direction $\hat{p} = \hat{x}$ and its perpendicular and longitudinal lengths b and L respectively. The inward heat flux q_0 flows along the x direction and is implemented at $x = 0$. The initial temperature is T_0 and it is the fixed temperature at $x = L$. The other surfaces are thermal insulators.

the quantitative influence of essential aspects, avoiding the complex implementation of an algebraic analysis. We implement simulations for the polar phase with $\hat{p} = \hat{n} = \hat{x}$ (see Fig. 2), using the standard case of 5CB [41] to fill a 10 μm cube, with the initial temperature $T_0 = 293.15$ K, inward heat flux q_0 along the x direction applied at $x = 0$, and exit temperature $T_{\text{out}} = T_0$ at $x = 10 \mu\text{m}$, with thermal insulation on the other surfaces. Instead of a temperature difference ΔT , we used in the simulation an inward heat flux q_0 with an opposite

temperature T_0 . This was done to highlight the technological application of inward solar radiation through the FNLC film on a glass window of a room with temperature T_0 . We solved the Fourier law $\nabla \cdot \mathbf{q} = 0$ with $q^i = -k^{ij}T_j$, with

$$k^{ij} = k_o^{ij} + a_0 A^{ijk} T_k. \tag{1}$$

Implementing this simulation and reversing where q_0 and T_0 are applied, we confirmed the algebraic results: there is a nonsymmetrical heat conduction along the director \hat{n} (collinear to p), in which $-p$ is the direction in which heat flows easily.

The term a_0 on Eq. (1) gives the “strength” of the polar phase, like the macroscopic magnitude of p , and it is also a parameter between the rank-3 tensor and the ordinary Fourier’s law to preserve the physical units, directly influencing the rectification efficiency. Thus, Fig. 3(a) shows the action of a_0 on the thermal contrast ratio. One sees that increasing a_0 , the contrast ratio $R = 1 - |\frac{q_R}{q_F}|$ rises because a_0 is also a measurement of the octupolar influence on the thermal conductivity tensor k^{ij} . Thus, enhancing the quality of the polar phase, i.e., the percentage of molecules in the polar state V , the thermal rectification intensifies, with a_0 playing a role similar to the scalar order parameter S [26,42]. Since p can be used as vector order parameter [7], and noting that both the p and the rank-3 tensor A_{ijk} exist only in the ferroelectric nematic phase, one expects $a_0 \propto |p|$. Thus, the maximum parameter a_0 will occur at the maximum $|p|$. For the DIO, where the nematic-to-ferroelectric nematic phase transition temperature is around 44 $^\circ\text{C}$ [19], the maximum a_0 will happen around 49 $^\circ\text{C}$, together with the maximum $|p|$.

Another critical aspect, particularly for the glass window industry or domestic customers, is knowing how much the

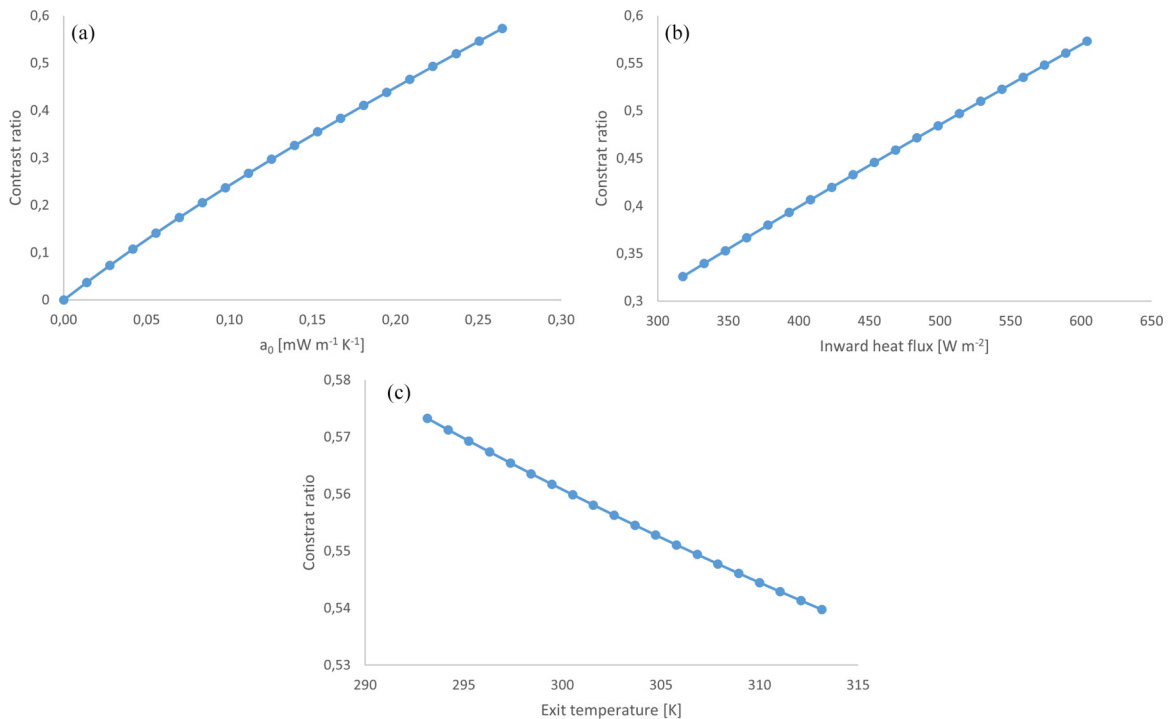


FIG. 3. Contrast ratio versus (a) parameter a_0 , (b) inward heat flux q_0 , and (c) exit temperature T_{out} .

rectification varies when the inward heat flux q_0 changes. Figure 3(b) shows how the contrast ratio changes with the inward heat flux. One observes that as q_0 increases, the contrast ratio increases, meaning the material is thermally more nonsymmetric along p as the available heat flux increases due to the nonlinear terms in Eq. (1) from the rank-3 tensor [22]. In a realistic case, the available heat flux will increase the local temperature, decreasing the local scalar order parameter and lowering the contrast ratio. Such temperature gain could induce, for example, the invariance of the contrast ratio for the inward heat flux, as it happens in nematic liquid-crystalline thermal diodes [36,37].

While the inward heat flow through a glass window varies, for example, with the changing seasons, electric devices can control the local indoor temperature, altering the efficiency of the contrast ratio. Figure 3(c) shows how the contrast ratio depends on the exit temperature T_{out} . One observes that by either increasing T_{out} or the temperature difference $T_{\text{out}} - T_0$, the contrast ratio decreases. The decrease in the contrast ratio is that the inward heat flux q_0 on the surface produces a temperature higher than T_{out} , and increasing T_{out} will decrease the difference in the temperature between the inward and outward surfaces, diminishing the thermal rectification effect. However, the drop in the contrast ratio is weak, emphasizing its thermal robustness against external disturbances compared to other microstructured thermal rectifiers [43]. Subsequently, such robustness on the one-directional heat flux [44] can improve the efficiency of solar refrigerators [45].

D. Geometric aspects of the simulations

When scaling thermal rectification for large dimensions, it is important to consider the development of technological applications on surfaces. To study that, we studied how the contrast ratio varies, changing the perpendicular length b , and the thickness L , with regards to the polar direction $\hat{p} = \hat{n} = \hat{x}$. We observe that the contrast ratio remains nearly constant, i.e., close to 0.6 regardless of the values of b and L , a result different from the other thermal diodes [24,35,37] where the rectification comes from the particular director field, while for FNLC it is an intrinsic property of the polar phase. This invariance is because the nonsymmetric heat conduction is an inherent material effect, as in Ref. [31], and not a product from a specific director field. Also, the decrease in the contrast ratio at the sixth decimal place is due to the automatic mesh thickening in response to the increase in b and L [46]. One can apply this feature to develop smart thermal resistances for interfaces [44].

IV. CONCLUSIONS

In this article, we used a rank-3 tensor approach to describe the $C_{\infty v}$ symmetry of FNLCs and its physical properties in

the polar phase. Due to the polar symmetry, nonsymmetric heat conduction rises along the direction of the polar vector \mathbf{p} , with the forward heat direction being $-\mathbf{p}$. Our simulations studied the influence of the term a_0 from the rank-3 approach on the thermal conductivity, the nonlinear Fourier's law, and the rectification efficiency of a thermal rectifier. Another critical aspect, particularly for the glass window industry or domestic customers, is knowing how much the rectification varies when the inward heat flux q_0 changes. The simulations also exposed the impact of the FNLC layer's thickness and exit temperature on the thermal rectification, and the results were summarized in graphs. We confirmed this result from the simulations measuring the heat contrast ratio R , and we noticed that R is directly proportional to the polar phase parameter a_0 and the inward heat flux q_0 , and inversely to the exit temperature T_0 . The reason is that a_0 works effectively as an order parameter of the polar phase. More inward heat flux means more heat to rectify, and the exit temperature also rules the available heat flux through the temperature difference between the inward and outward surfaces. Relative to the bulk geometry of the polar phase, the contrast ratio does not change substantially when we alter the dimensions of the sample, meaning the translation symmetry breaking for heat is an intrinsic feature of the polar phase. These results might provide useful insights for suitable technological applications. For example, an FNLC film applied on glass windows will increase its contrast ratio adaptively if the inward heat flux increases, and thus it keeps rectifying even for thin layers, saving materials in manufacturing processes. In future works, we can explore the influence of such nonsymmetrical thermal conductivity under the presence of conic defects [47] and study the translation symmetry breaking for light propagation.

The data that support the findings of this study are available from the corresponding author upon reasonable request.

ACKNOWLEDGMENTS

The authors acknowledge the Conselho Nacional de Desenvolvimento Científico e Tecnológico (CNPq), the Coordenação de Aperfeiçoamento de Pessoal de Nível Superior (CAPES), the Fundação de Amparo à Ciência e Tecnologia do Estado de Pernambuco (FACEPE), the Instituto Nacional de Ciência e Tecnologia de Fluidos Complexos (INCT-FCx), and the Fundação de Amparo à Pesquisa do Estado de São Paulo (2014/50983-3) (FAPESP-2014/50983-3).

L.M.S. performed formal analysis, investigation, software, visualization, writing the original draft and review and editing. J.S. was responsible for formal analysis, visualization, writing the original draft and review and editing. E.P. handled conceptualization, formal analysis, investigation, methodology, project administration, software, supervision, visualization, writing the original draft and review and editing.

There are no conflicts of interest to declare.

[1] J. Beekman, Liquid-crystal photonic applications, *Opt. Eng.* **50**, 081202 (2011).

[2] M. Bremer, P. Kirsch, M. Klasen-Memmer, and K. Tarumi, The TV in your pocket: development of liquid-crystal materials

for the new millennium, *Angew. Chem. Int. Ed.* **52**, 8880 (2013).

[3] J. Mysliwiec, A. Szukalska, A. Szukalski, and L. Sznitko, Liquid crystal lasers: The last

- decade and the future, *Nanophotonics* **10**, 2309 (2021).
- [4] H. Kawamoto, The history of liquid-crystal displays, *Proc. IEEE* **90**, 460 (2002).
- [5] D.-K. Yang and S.-T. Wu, *Fundamentals of Liquid Crystal Devices* (John Wiley, New Jersey, 2006).
- [6] O. D. Lavrentovich, Ferroelectric nematic liquid crystal, a century in waiting, *Proc. Natl. Acad. Sci. USA* **117**, 14629 (2020).
- [7] N. Sebastián, M. Čopič, and A. Mertelj, Ferroelectric nematic liquid-crystalline phases, *Phys. Rev. E* **106**, 021001 (2022).
- [8] E. I. Kats, Stability of the uniform ferroelectric nematic phase, *Phys. Rev. E* **103**, 012704 (2021).
- [9] Q. Guo, K. Yan, V. Chigrinov, H. Zhao, and M. Tribelsky, Ferroelectric liquid crystals: Physics and applications, *Crystals* **9**, 470 (2019).
- [10] A. K. Srivastava, V. G. Chigrinov, and H. S. Kwok, Ferroelectric liquid crystals: Excellent tool for modern displays and photonics, *J. Soc. Inf. Disp.* **23**, 253 (2015).
- [11] A. Kumar, Priyam, H. Meena, J. Prakash, L. Wang, and G. Singh, Recent advances on semiconducting nanomaterials–ferroelectric liquid crystals nanocomposites, *J. Phys.: Condens. Matter* **34**, 013004 (2022).
- [12] A. Kumar, J. Prakash, A. M. Biradar, and W. Haase, Abiding electro-optic memory effect based on deformed helix ferroelectric liquid crystal, *Appl. Phys. Express* **3**, 091701 (2010).
- [13] Y. Lin, G. Li, P. Yu, E. Ercan, and W. Chen, Organic liquid crystals in optoelectronic device applications: Field-effect transistors, nonvolatile memory, and photovoltaics, *J. Chin. Chem. Soc.* **69**, 1289 (2022).
- [14] S. Marni, G. Nava, R. Barboza, T. G. Bellini, and L. Lucchetti, Walking ferroelectric liquid droplets with light, *Adv. Mater.* **35**, 2212067 (2023).
- [15] M. T. Máthé, Á. Buka, A. Jákli, and P. Salamon, Ferroelectric nematic liquid crystal thermomotor, *Phys. Rev. E* **105**, L052701 (2022).
- [16] L. Cmok, V. Coda, N. Sebastian, A. Mertelj, M. Zgonik, S. Aya, M. Huang, G. Montemezzani, and I. Drevenšek-Olenik, Running streams of a ferroelectric nematic liquid crystal on a lithium niobate surface, *Liquid Crystals* **50**, 1478 (2023).
- [17] J. Li, H. Nishikawa, J. Kougo, J. Zhou, S. Dai, W. Tang, X. Zhao, Y. Hisai, M. Huang, and S. Aya, Development of ferroelectric nematic fluids with giant- ϵ dielectricity and nonlinear optical properties, *Sci. Adv.* **7**, eabf5047 (2021).
- [18] J. Li, Z. Wang, M. Deng, Y. Zhu, X. Zhang, R. Xia, Y. Song, Y. Hisai, S. Aya, and M. Huang, General phase-structure relationship in polar rod-shaped liquid crystals: Importance of shape anisotropy and dipolar strength, *Giant* **11**, 100109 (2022).
- [19] H. Nishikawa, K. Shiroshita, H. Higuchi, Y. Okumura, Y. Haseba, S. Yamamoto, K. Sago, and H. Kikuchi, A fluid liquid-crystal material with highly polar order, *Adv. Mater.* **29**, 1702354 (2017).
- [20] R. J. Mandle, S. J. Cowling, and J. W. Goodby, Rational design of rod-like liquid crystals exhibiting two nematic phases, *Chem. Eur. J.* **23**, 14554 (2017).
- [21] R. J. Mandle, S. J. Cowling, and J. W. Goodby, A nematic to nematic transformation exhibited by a rod-like liquid crystal, *Phys. Chem. Chem. Phys.* **19**, 11429 (2017).
- [22] T. C. Lubensky and L. Radzihovsky, Theory of bent-core liquid-crystal phases and phase transitions, *Phys. Rev. E* **66**, 031704 (2002).
- [23] A. Jákli, O. D. Lavrentovich, and J. V. Selinger, Physics of liquid crystals of bent-shaped molecules, *Rev. Mod. Phys.* **90**, 045004 (2018).
- [24] J. G. Silva, S. Fumeron, F. Moraes, and E. Pereira, High thermal rectifications using liquid crystals confined into a conical frustum, *Braz. J. Phys.* **48**, 315 (2018).
- [25] W. K. P. Barros and E. Pereira, Concurrent guiding of light and heat by transformation optics and transformation thermodynamics via soft matter, *Sci. Rep.* **8**, 11453 (2018).
- [26] S. Fumeron, F. Moraes, and E. Pereira, Thermal and shape topological robustness of heat switchers using nematic liquid crystals, *Eur. Phys. J. E* **41**, 16 (2018).
- [27] D. Frenkel, Entropy-driven phase transitions, *Phys. A (Amsterdam, Neth.)* **263**, 26 (1999).
- [28] G. B. Arfken, H. J. Weber, and F. E. Harris, *Mathematical Methods for Physicists: A Comprehensive Guide* (Academic, New York, 2013).
- [29] N. Li, J. Ren, L. Wang, G. Zhang, P. Hanggi, and B. Li, *Colloquium: Phononics: Manipulating heat flow with electronic analogs and beyond*, *Rev. Mod. Phys.* **84**, 1045 (2012).
- [30] J.-X. Wang, P. Birbarah, D. Docimo, T. Yang, A. G. Alleyne, and N. Miljkovic, Nanostructured jumping-droplet thermal rectifier, *Phys. Rev. E* **103**, 023110 (2021).
- [31] C. W. Chang, D. Okawa, A. Majumdar, and A. Zettl, Solid-state thermal rectifier, *Science* **314**, 1121 (2006).
- [32] N. Yang, G. Zhang, and B. Li, Thermal rectification in asymmetric graphene ribbons, *Appl. Phys. Lett.* **95**, 33107 (2009).
- [33] X. Yang, S. Wang, C. Wang, R. Lu, X. Zheng, T. Zhang, M. Liu, J. Zheng, and H. Chen, Thermal rectifier and thermal transistor of 1T/2H MoS₂ for heat flow management, *ACS Appl. Mater. Interfaces* **14**, 4434 (2022).
- [34] Y. Zhang, C.-L. Zhou, H.-L. Yi, and H.-P. Tan, Radiative thermal diode mediated by nonreciprocal graphene plasmon waveguides, *Phys. Rev. Appl.* **13**, 034021 (2020).
- [35] D. Melo, I. Fernandes, F. Moraes, S. Fumeron, and E. Pereira, Thermal diode made by nematic liquid crystal, *Phys. Lett. A* **380**, 3121 (2016).
- [36] S. J. Santos, J. Andrade, and E. Pereira, Simultaneous rectification of heat and light using liquid crystal, *J. Appl. Phys.* **124**, 094501 (2018).
- [37] V. Silva, E. Pereira, F. Moraes, and S. Fumeron, Thermal rectification film using liquid crystalline asymmetric diodes, *Braz. J. Phys.* **51**, 1636 (2021).
- [38] G. Dai and J. Huang, Nonlinear thermal conductivity of periodic composites, *Int. J. Heat Mass Transfer* **147**, 118917 (2020).
- [39] B. Li, L. Wang, and G. Casati, Thermal diode: Rectification of heat flux, *Phys. Rev. Lett.* **93**, 184301 (2004).
- [40] L. Wang, B. Hu, and B. Li, Logarithmic divergent thermal conductivity in two-dimensional nonlinear lattices, *Phys. Rev. E* **86**, 040101(R) (2012).
- [41] G. Ahlers, D. S. Cannell, L. I. Berge, and S. Sakurai, Thermal conductivity of the nematic liquid crystal 4-*n*-pentyl-4'-cyanobiphenyl, *Phys. Rev. E* **49**, 545 (1994).

- [42] P. G. de Gennes and J. Prost, *The Physics of Liquid Crystals* (Clarendon, Oxford, 1992).
- [43] M. Schmotz, J. Maier, E. Scheer, and P. Leiderer, A thermal diode using phonon rectification, *New J. Phys.* **13**, 113027 (2011).
- [44] J. Chen, X. Xu, J. Zhou, and B. Li, Interfacial thermal resistance: Past, present, and future, *Rev. Mod. Phys.* **94**, 025002 (2022).
- [45] D. S. Kim and C. A. Infante Ferreira, Solar refrigeration options—a state-of-the-art review, *Int. J. Refrig.* **31**, 3 (2008).
- [46] COMSOL Inc., *COMSOL Multiphysics 5.6 Reference Manual* (Stockholm, Sweden, 2020).
- [47] P. Kumari, B. Basnet, H. Wang, and O. D Lavrentovich, Ferroelectric nematic liquids with conics, *Nat. Commun.* **14**, 748 (2023).